Eur. Phys. J. D **23**, 73–79 (2003)
DOI: 10.1140/epjd/e2003-00051-7

THE EUROPEAN PHYSICAL JOURNAL D

Cascade feeding of the 1s3d ^{3}D level of He I from high-l states excited by proton impact

R. Drozdowski[a]

University of Gdańsk, Institute of Experimental Physics, ul. Wita Stwosza 57, 80-952 Gdańsk, Poland

Received 15 October 2001 / Received in final form 26 July 2002
Published online 4 March 2003 –

Abstract. The $1s3d\ ^3$D level of atomic helium cannot be excited directly by proton impact, but it is strongly populated by cascade feeding from $1snl$ states with $l \geq 3$, if $10 \div 15$ keV protons are used for excitation. This cascade feeding process can be analysed in detail by investigating the intensity of the spectral line at $\lambda(1s3d\ ^3\mathrm{D}–1s2p\ ^3\mathrm{P}) = 588$ nm as a function of an electric field directed parallel and antiparallel to the proton beam. In this paper the intensity functions are calculated assuming collisional excitation of parabolic singlet states $|1s; n, n_1, n_2, m\rangle$ with large electric dipole moments. The theoretical results are compared with the experimental intensity function published earlier. Excellent agreement is obtained if the excitation cross-sections σ_n of the parabolic states scale as n^{-3}.

PACS. 34.50.-s. Scattering of atoms and molecules – 32.60.+i Zeeman and Stark effects

1 Introduction

Studying ion-atom collisions provides an opportunity to analyze the dynamics of atomic processes. Here we are concerned with proton-impact excitation of helium atoms. In the spectrum of He atoms excited by collisions with protons strong triplet lines are observed, though according to Wigner's spin conservation rule one expects that only singlet states are excited. It has been shown [1] that an excitation of triplet states is possible due to the strong singlet-triplet mixing occurring in He I $1snl$ states with $l \geq 3$ [2]. For analyzing the appearance of triplet lines, it is convenient to describe the excitation process using excitation matrices. It is a Hermitian matrix. The (real) diagonal matrix elements are the excitation cross-sections of the basis states used for the matrix representation of the excitation operator, and the complex off-diagonal elements are coherence parameters describing the coherent excitation of different basis states. Their real components are related to the charge distribution [3,4] and their imaginary components to the current distribution [5] of the post-collisional atomic state. The coherence parameters can be determined experimentally by measuring the fluorescence-light intensity of spectral lines if specially designed electric and magnetic fields are applied to the collision volume.

In this paper I investigate the appearance of the He I triplet line $\lambda(1s3d\ ^3\mathrm{D}–1s2p\ ^3\mathrm{P}) = 588$ nm after collisional excitation of He atoms by proton impact. The occurrence of this spectral line is surprising, because the singlet-triplet mixing of the $1s3d$ levels is extremely small. However, cascade feeding of the $1s3d\ ^3$D level is possible, if $l \geq 3$ states are populated by the excitation process. Aynacioglu *et al.* [6] have shown that, indeed, cascade feeding from $l \geq 3$ states is the dominant excitation mechanism for excitation of the $1sd\ ^3$D level by proton impact. Therefore, the appearance of the 588 nm line provides a unique opportunity for studying the excitation of the high-l states of He I by proton impact. As has been shown by Aynacioglu *et al.*, an excitation of high-l states is most likely at intermediate energies, where the velocity v_p of the proton is on the order of the Bohr velocity $v_\mathrm{B} = 1$ a.u.

The significance of cascade feeding for the excitation of the $1snd\ ^3$D levels by proton impact becomes obvious also from measurements of Büttrich *et al.* [7], in which the excitation of the $1snd\ ^1$D levels has been investigated using anticrossing techniques. They measured the intensities $I_\lambda(F_z)$ of the $\lambda(1snd - 1s2p\ ^3\mathrm{P})$ spectral lines as a function of an electric field F_z applied to the collision volume parallel and antiparallel to the proton beam. Though experimental recordings $I_\lambda(F_z)$ were published in [7] only for the $1snd$ configurations with $n = 4 \div 7$, they also recorded an intensity function of the $1s3d\ ^3$D–$1s2p\ ^3$P transition. However, the electric fields, which could be applied, were too weak for reaching the singlet-triplet anticrossings of the $1s3d$ configuration. Therefore, this measurement was left out of consideration in [7]. But a recording of the intensity function of the 588 nm line has been published by Skogvall and von Oppen [8]. These authors emphasize the relation of the intensity variations near zero-field to cascade feeding of the $1s3d\ ^3$D level, but do not present a detailed evaluation of this recording either.

[a] e-mail: fizrd@univ.gda.pl

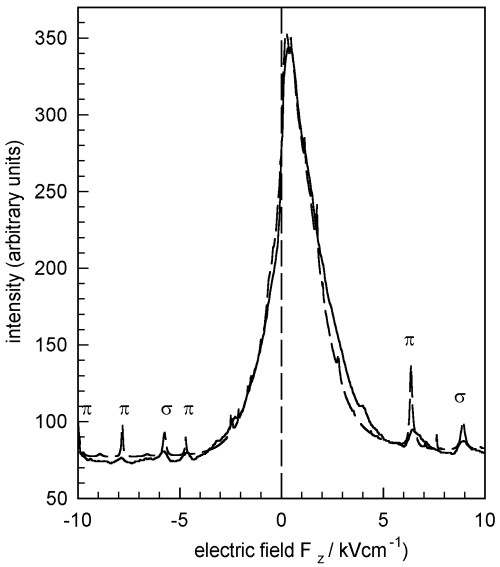

Fig. 1. The intensity function $I_{588}(F_z)$ of the $\lambda(1s3d\ ^3\mathrm{D}$–$1s2p\ ^3\mathrm{P}) = 588$ nm line for 12.5 keV proton-impact excitation of helium atoms. The solid curve is the recorded [8] experimental shape, the broken curve represents the theoretical result.

Nevertheless, this recording, which is reproduced in Figure 1, is worthwhile to be thoroughly evaluated. It gives detailed information about the excitation of $l \geq 3$ states of He I by 12.5 keV-proton impact and the relative contributions of the various $1snl$ configurations to cascade feeding. This information is of great interest with respect to a better understanding of the excitation mechanisms dominating in ion-atom collisions at intermediate energies. In particular, regarding proton-helium collisions, a Paul-trap model has been proposed for explaining the resonance structure in the excitation functions of the $1snd\ ^1\mathrm{D}$ levels at impact energies E_p between 10 and 15 keV [12]. This excitation mechanism implies that also high-l states are strongly populated in this energy region.

In this paper I investigate the cascade feeding of the $1snd\ ^3\mathrm{D}$ level after selective excitation of singlet states theoretically. The measured intensity function of the 588 nm line, in particular, its asymmetry can be explained by assuming that the $1snl$ states with $n \leq 7$ are populated in agreement with the Paul-trap model and that the excitation cross-sections scale as n^{-3}.

2 Collisional excitation and radiative decay in electric fields

In the semiclassical approach to ion-atom collisions the projectile and target nucleus are assumed to move on classical trajectories. Therefore, their relative motion can be parameterized by the impact parameter b and the angle φ of the scattering plane. Accordingly, scattering, excitation and charge transfer can be described as processes depending on b and φ. The evolution of the electron cloud during the collision is evaluated quantum dynamically. As a result of this evolution, the post-collisional states $\Psi_n(b,\varphi)$ of *e.g.* a target atom with an electron excited to an orbit with principal quantum number n is a pure state:

$$|\psi_n(b,\varphi)\rangle = \sum_{LSJM} |n(LS)JM\rangle\langle n(L,S)JM|\psi_n(b,\varphi)\rangle$$
$$= \sum_{LSJM} a_{nLSJM}(b,\varphi)|n(LS)JM\rangle\cdot \qquad (1)$$

In integral experiments, where atoms are observed regardless of the parameters (b,φ) of the relative motion of the collision system, the ensemble of excited atoms is in a mixed state described by a density matrix σ, usually called excitation matrix. The matrix elements $\sigma_{kk'}$ are obtained from the density matrices describing the pure states $\psi_n(b,\varphi)$ by integrating over the parameters b and φ:

$$\sigma_{kk'} = \int_0^{2\pi}\int_0^{\infty} a_k(b,\varphi)a_{k'}^*(b,\varphi)b\,\mathrm{d}b\,\mathrm{d}\varphi \qquad (2)$$

where k, k' denote the quantum numbers n, l, m of the orbital basis states $|n,l,m\rangle$ used for the representation of the excitation matrix.

Due to the integration over φ, the excitation matrix is rotationally symmetric. Therefore, states with different Zeeman quantum numbers m are populated incoherently, that is the off-diagonal matrix elements of σ with $m \neq m'$ vanish. Regarding the integration over the impact parameter b, the question arises, to which extent this integration implies that also states with different angular momentum quantum numbers l are populated incoherently.

Actually, considering proton-helium collisions at intermediate energies, not only states with low l quantum numbers as for high-energy collisions, but also the high-angular momentum states are strongly populated. Surprisingly, it could be shown experimentally that all states of an n shell differing only in l are populated highly coherently. The experimental investigations performed by Büttrich and von Oppen [9] even more revealed that the post-collisional n-shell states are the parabolic states $|n;n_1,n_2,m\rangle$ with $n_2 = 0$ and $|m| = 0$ and 1. This highly selective excitation of states with large electric dipole moments occurs especially in the energy range 10 keV $< E_p <$ 15 keV, where the excitation cross-sections exhibit a resonance-like maximum. To explain this maximum, the Paul-trap model was proposed [10–12]. According to this model, the rotation of the molecular axis of the collision system is essential for excitation at intermediate energies. During the collision, one electron of the He atom is energetically promoted on the saddle of the two-center field of the ionic projectile and the singly charged core of the target atom. This promotion on the saddle is most effective at intermediate energies due to the rotation of the collision system, which stabilizes the electron's motion on the saddle as in a Paul-trap [13].

The evolution of the electron cloud on the saddle of the two-center field during the final phase of the collision can be treated within the framework of saddle dynamics introduced by Rost and Briggs [14]. They consider the symmetrical two-center potential of the H_2^+ system. According to saddle dynamics, the saddle state evolves diabatically

along the in-saddle sequences to parabolic separated-atom states with n_1 or $n_2 = 0$. Starting from the molecular ground state $1s\sigma_g$ the electron is promoted along the in-saddle sequence $1s\sigma$–$3d\sigma$–$5g\sigma$... This sequence leads to the parabolic target states $|n; n-1, 0, 0\rangle$. On the other hand, if the collision starts in the $2p\sigma$ state, the collision system can evolve after a rotational $2p\sigma$–$2p\pi$ coupling along the sequence $2p\pi$–$4f\pi$–$6h\pi$... This sequence leads to the parabolic target states $|n; n-2, 0, \pm 1\rangle$. Besides direct excitation of target atoms, also electron transfer leading to excited projectile atoms is possible. Saddle dynamics leads also to parabolic post-collisional projectile states, but that are states with $n_1 = 0$. Here we assume a z-axis parallel to the ion beam. According to these excitation processes one expects that the electric dipole moments $\langle -ez \rangle$ of the post-collisional target states are not only non-zero, but also extremely large. For parabolic states these expectation values are given by [15]:

$$\langle -ez \rangle = -\frac{3}{2} n (n_1 - n_2) \text{ a.u.} \tag{3}$$

Large electric dipole moments were detected first by Havener *et al.* [16] for hydrogen atoms excited by electron transfer in H^+–He collisions with respect to single-electron excitation, this collision system is similar to H_2^+. One electron can be assumed to stay as a spectator in the $1s$ orbital during the collision. Therefore, saddle dynamics is likely to provide a simple intuitive model for explaining the large values of the experimentally measured electric dipole moments.

As expected according to saddle dynamics, not only the post-collisional projectile states investigated by Havener *et al.*, but also the post-collisional target states have large electric dipole moments, though with opposite sign. This was shown by the measurements of Büttrich *et al.* [7]. They used an experimental setup described in [17]. A well collimated proton beam is crossed with a thermal beam of helium atoms effusing from a multichannel plate. An electric field F_z could be applied to the collision region parallel ($F_z > 0$) and antiparallel ($F_z < 0$) to the ion beam. The fluorescence light emitted after collisional excitation in a direction perpendicular to ion and atom beam was detected using a photomultiplier. The intensity of spectral lines selected with interference filters were measured as a function of the electric field applied to the collision region. Using this experimental technique, also the intensity function $I_{588}(F_z)$ of the $\lambda(1s3d\ ^3\text{D}$–$1s2p\ ^3\text{P}) = 588$ nm line of He I shown in Figure 1 was recorded.

This intensity function, in particular, the remarkable decrease of the intensity at electric fields of a few kV/cm indicates that the $1s3d\ ^3$D level is dominantly populated by cascade feeding from high-l states. At zero-field this excitation process is highly effective, because the $1s3d\ ^3$D level is the energetically lowest $l = 2$-level, to which the atoms excited to states with $l \geq 3$ can cascade down. However, at electric fields of a few kV/cm the nl states with $l \geq 3$ are strongly mixed with the nd states and, therefore, they decay preferentially directly to the $1s2p$ configuration. In addition, also due to the Stark mixing with the nd states, the singlet-triplet mixing of the high-l states is strongly reduced by applying electric fields. Therefore, transitions between singlet and triplet states are suppressed and, hence, the population of triplet states by cascade feeding, since the post-collisional He I states excited by proton impact are singlet states.

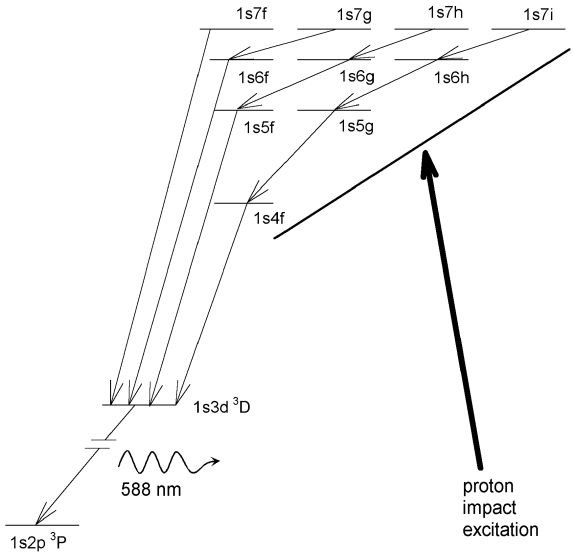

Fig. 2. The energy levels scheme for He atom with indicated possible cascade transitions feeding the $1s3d\ ^3$D level.

Further remarkable features of this intensity function are its asymmetry and the small intensity maxima at non-zero electric fields. The asymmetry reflects the asymmetry of the charge distributions of the post-collisional He I states. The side maxima are due to singlet-triplet anticrossings of the $1s5l$ configurations. The occurrence of these anticrossing resonances immediately indicates that not only the $1s4f$ configuration, but also the $1s5l$ states contribute to cascade feeding of the $1s3d\ ^3$D level.

The level scheme of He I shown in Figure 2 illustrates cascade feeding of the $1s3\ ^3$D level from all $1snl$ configurations with $n \leq 7$. These cascade channels were taken into account below to explain the measured intensity function theoretically. Cascade feeding from high-n states has a significant effect on the shape of the intensity function at weak electric fields, because the polarizability of excited He atom scales as n^5.

3 Quantitative evaluation of $I_{588}(F_z)$

The population of the $1s3d\ ^3$D states by cascade feeding in an axial electric field can be evaluated quantitatively using rate equations [8,18,19] describing excitation and decay of all Stark sublevels k involved in the cascade processes:

$$I_p \sigma_k + \sum_i W_{ik} P_i - \Gamma_k P_k = 0. \tag{4}$$

The collisional excitation rate $I_p \sigma_k$ depends on the intensity I_p of the proton beam (number of protons per m^2 s)

and the excitation cross-section

$$\sigma_k = \langle k|\sigma|k\rangle$$

of the eigenstate $|k\rangle$ of the Stark sublevel. The rate for cascade feeding from an energetically higher Stark state $|i\rangle$ with population number P_i is given by the product $W_{ik}P_i$, where [15]

$$W_{ik} = \frac{4}{3}\frac{e^2\varpi_{ik}^3}{\hbar c^3}\,|r_{ik}|^2 \tag{5}$$

is the rate of spontaneous transitions from $|i\rangle$ to $|k\rangle$ due to the electric dipole coupling of the atom to the radiation field ($e^2/\hbar c = \alpha$ fine structure constant, ϖ_{ik} transition frequency). Under stationary conditions collisional excitation and cascade feeding of the Stark substate $|k\rangle$ is balanced by its radiative decay given by the decay rate $\Gamma_k = \sum_i W_{ki}$ and the population number P_k of $|k\rangle$.

The population numbers P_k can be calculated using rate equation (4) provided coherence between the population amplitudes of different Stark substates can be neglected. This assumption is justified, since (i) the thermal motion of the excited He atoms is negligible and (ii) an axial electric field is applied. Due to condition (i), excitation and decay takes place under stationary conditions and, therefore, coherence between the population amplitudes of non-degenerate Stark states can be disregarded. Degenerate Stark states, however, have different Zeeman quantum numbers m. Therefore, one finds in this case $\langle k|\sigma|k'\rangle = 0$, if the electric field is parallel to the proton beam.

The population numbers P_k can be deduced from the rate equations, if the excitation cross-sections σ_k, the transition rates W_{ik} and the decay rates Γ_k are known. These parameters are functions of the electric field strength. However, it can reasonably be assumed that the electric-field dependence is exclusively a result of the fact that the eigenstates $|k\rangle$ of the Stark sublevels change with the strength of the electric field F_z.

Regarding the excitation cross-sections σ_k, I assume that the collisional excitation process taking place in a time

$$\tau_{\rm coll} \ll \tau_{\rm evol} = \frac{\hbar}{E - E'}, \tag{6}$$

that is short compared with the evolution periods of n-shell states, is not affected by the strength of the external field and the internal magnetic fine-structure coupling. In that case, an electric-field independent excitation matrix $\sigma^{(n)}$ can be introduced, which describes the ensemble of atoms excited to n-shell states immediately after collisional excitation. Using a representation with Russell-Saunders basis states $|n(LS)J, m\rangle$ it has the following properties:

(i) because of Wigner's spin conservation rule, only singlet states can be excited by proton impact, that is only matrix elements with $S = S' = 0$ are non-zero;
(ii) due to the rotational symmetry with respect to the proton beam, only matrix elements with $m = m'$ are non-zero;
(iii) because of the reflection symmetry with respect to any plane containing the beam, the matrix elements are independent of the sign of m.

In spite of these restrictions, the excitation matrix $\sigma^{(n)}$ is still a function of a set of $\sum_{v=1}^{n} v^2 = n(n+1)(2n+1)/6$ independent (real) parameters determined by the dynamics of the excitation process. Assuming that the excitation of He atoms by 12.5 keV-proton impact is dominated by saddle dynamics, the number of dynamical parameters is reduced to 2, namely the excitation cross-sections of the parabolic singlet states $^1\Sigma$ and $^1\Pi$, where the excited electron is in a state $|n; n_1, n_2, m\rangle$ with $n_2 = 0$ and $|m| = 0$ or 1. Indeed, assuming this highly selective excitation mechanism, the cascade feeding of the $1s3d$ ^{3}D level can be explained in good agreement with the measured intensity function $I_{588}(F_z)$ shown in Figure 1.

For determining the contributions of the different n shells to the cascade feeding of the $1s3d$ ^{3}D level, the electric field dependent eigenstates $|k\rangle$ of the He atom and the transition rates W_{ik} defined in (5) have to be calculated. That was done by diagonalizing the Hamiltonian

$$H = H_0 + H_{\rm el}, \tag{7}$$

composed of the zero-field Hamiltonian H_0 of the He atom and the interaction of the atom with the external electric field

$$H_{\rm el} = ezF_z. \tag{8}$$

For each n shell the submatrices $H^{(n)}$ were diagonalized separately. The matrix elements of $H_0^{(n)}$ in Russell-Saunders representation were deduced from the experimental level energies [20] using the approach of Cok and Lundeen [2] to reproduce the fine structure of the $1snl$ configurations. The parameters $h_{\rm off}$ of the off-diagonal matrix elements of the spin-orbit coupling are essential for the formation of singlet-triplet anticrossings, however, they cannot be deduced from the measured fine-structure separations independently of the other fine-structure parameters. Therefore, the parameters $h_{\rm off}$ were calculated using their relation to the parameters of the diagonal matrix elements of the spin-orbit coupling:

$$h_{\rm off} = 3h_{\rm so} \tag{9}$$

valid in the Heisenberg approximation. All parameters of $H_0^{(n)}$ used for diagonalizing $H^{(n)}$ were tabulated for $n = 2 \div 8$ by Kaiser [21] and partly (for $n = 3 \div 5$) by Kaiser *et al.* [22].

For evaluating the Hamiltonian $H_{\rm el}$ it is most appropriate to refer to the $|n; l, M_L, S, M_S\rangle$ basis, where $\mathbf{L}$ and $\mathbf{S}$ are decoupled. In that case $H_{\rm el}$ is diagonal in M_L, S and M_S, and the matrix elements of $H_{\rm el}$ are given by:

$$\langle n, L, M_L, S, M_S|H_{\rm el}|n', L', M_L, S, M_S\rangle = (-1)^{L-M_L}\begin{pmatrix} L' & 1 & L \\ -M_L & 0 & M_L \end{pmatrix}\langle nL \parallel \mathbf{r} \parallel n'L'\rangle eF_z. \tag{10}$$

The reduced matrix elements $\langle nL \parallel \mathbf{r} \parallel n'L'\rangle$ of the electric dipole operator $\mathbf{r}$ for S–P and P–D transitions are obtained from the oscillator strengths $f_{nLS}^{n'L+1S}$, calculated by Kono and Hattori [23]:

$$|\langle nL+1S \parallel \mathbf{r} \parallel n'LS\rangle|^2 = \frac{3(2L+1)}{2|E_{n'L+1S} - E_{nLS}|}|f_{nLS}^{n'L+1S}|, \tag{11}$$

where E_{nLS} denote the experimental ionization energy taken from Martin [24]. The signs of the reduced matrix elements are adopted from the hydrogen atom (see below).

The reduced matrix elements $\langle nL+1 \parallel \mathbf{r} \parallel n'L\rangle$ of $\mathbf{r}$ with $L \geq 2$ were calculated using the Heisenberg approximation given by Bethe and Salpeter [15], where $L = l$ is the angular momentum quantum number of the excited electron:

$$\langle n'l+1 \parallel \mathbf{r} \parallel nl\rangle = \sqrt{l+1}R_{nl}^{n'l+1}. \tag{12}$$

In that case, the radial integrals $R_{nl}^{n'l'}$ for $n = n'$ needed for evaluating the matrix elements of H_{el} are given by:

$$R_{nl}^{nl-1} = R_{nl-1}^{nl} = \frac{3}{2}n\sqrt{n^2 - l^2}. \tag{13}$$

The radial integrals $R_{nl}^{n'l'}$ for $n \neq n'$ needed for evaluating the radiative transition rates W_{ik} according to formula (5) are also given by Bethe and Salpeter. Using these matrix elements of the electric dipole operator $\mathbf{r}$, the transition matrix elements $\mathbf{r}_{ik}$ between the electric-field eigenstates and the transition rates W_{ik} as well as the decay rates Γ_k can be evaluated. With these calculated parameters and the known eigenstates $|k\rangle$ of the Hamiltonian (7) the population probabilities P_k were calculated from (4) as functions of the electric field F_z using an appropriate assumption for the excitation matrices $\sigma^{(n)}$. With respect to proton-impact excitation of He atoms within the energy range of the resonance structure between 10 and 15 keV it is reasonable to assume selective excitation of the parabolic states $|n; n_1, n_2, m\rangle$ with $n_2 = 0$ and $|m| = 0$ or 1 in accordance with saddle dynamics. In that case, the relative excitation cross-sections of these states are the only variables available for fitting the measured intensity functions $I_\lambda(F_z)$ theoretically.

Büttrich *et al.* [7] have shown that within the $n = 5$ shell the two parabolic states $|5; 4, 0, 0\rangle$ and $|5; 3, 0, \pm 1\rangle$ are populated approximately in the ratio 1.5 : 1 and that similar results are found for the shells with $n = 4$ to 8. Using these experimental ratios, the cascade contributions due to direct excitation of states with $n = 4$ to 7 to the population of the $1s3d\ ^3$D level were calculated as functions of the electric field F_z. Cascade contributions from states with $n \geq 8$ were disregarded.

Finally, using the calculated population probabilities $P_k^{(3)}$ of the $1s3d\ ^3$D Stark substates, the intensity function $I_{588}(F_z)$ of the detected 3 ^{3}D–2 ^{3}P transitions can be determined. The intensity function $I_{588}(F_z)$ was measured by detecting light emitted within a solid angle $\mathrm{d}\Omega$ perpendicular (y-direction) to the direction of the electric field F_z. Accordingly, the polarization $\mathbf{e}_j$ of the photons is $\mathbf{e}_x$ or $\mathbf{e}_z$. Therefore, the fraction $\mathrm{d}W_{ik}$ of the spontaneous emission rate W_{ik}, where a photon is emitted in the solid angle $\mathrm{d}\Omega$ is given by [15]:

$$\mathrm{d}W_{ik} = \left[e^2/(hc^3)\right]\omega^3\ \mathrm{d}\Omega \sum_{j=x,z}(\mathbf{e}_j\mathbf{r}_{ik})^2 \tag{14}$$

with

$$\sum_{j=x,z}(\mathbf{e}_j\mathbf{r}_{ik})^2 = |\langle i|x|k\rangle|^2 + |\langle i|z|k\rangle|^2. \tag{15}$$

With these emission rates the intensity function $I_{588}(F_z)$ is given by

$$I_{588}(F_z) = g_{588}N_T\sum_{ki}\mathrm{d}W_{ki}P_k, \tag{16}$$

where the summation $\sum_{ki}$ runs over all components of the $1s3d\ ^3$D–$1s2p\ ^3$P transition and g_{588} and N_T are proportionality constants representing the efficiency for detecting 588 nm photons and the number of target atoms in the collision volume, respectively.

4 Results and discussion

Assuming selective excitation of He I-singlet states, the $1s3d\ ^3$D level can only be populated by cascade feeding. Most likely is cascade feeding from $1s4f$ states. Figure 3 shows intensity functions $I_{588}(F_z)$ calculated for direct excitation of the parabolic $n = 4$ states $|4; n_1, n_2, m\rangle$ with $m = 0$ or 1 and $n_2 = 0$ (Figs. 3a and 3d) or $n_2 = 1$ (Figs. 3b and 3e). Asymmetric intensity functions with a maximum at an electric field $F_z > 0$ are obtained for states with $n_1 > n_2$, that is states with an asymmetric charge distribution. However, for excitation of the state $|4; 1, 1, 1\rangle$, where $n_1 = n_2$, the intensity function is symmetric. Also shown are the interference terms resulting from coherent excitation of the two parabolic states with $m = 0$ (Fig. 3c) and $m = 1$ (Fig. 3f). In these cases, the intensity function was calculated using an excitation matrix, where only the off- diagonal matrix elements $\langle k|\sigma|k'\rangle$ between the coherently excited states are non-zero. Therefore, since the excitation matrix is not positive definite, the intensity can be negative. Only a superposition of the calculated intensity functions corresponding to a positive definite excitation matrix is physically relevant.

The presented curves were calculated using the normalization $\mathrm{Tr}(\sigma) = 100$, if the excitation matrix is positive definite. For the interference terms ($k \neq k'$), where $\mathrm{Tr}(\sigma) = 0$, both off-diagonal elements were put $\langle k|\sigma|k'\rangle = \langle k'|\sigma|k\rangle = 100$. The intensity functions calculated for Π states include a weight factor 2 taking into account the $\pm m$ degeneracy of Stark sublevels.

The intensity functions calculated with the parabolic $n_1 = 0$ states qualitatively reproduce some features of the measured intensity function shown in Figure 1, in particular, the asymmetry of the zero-field

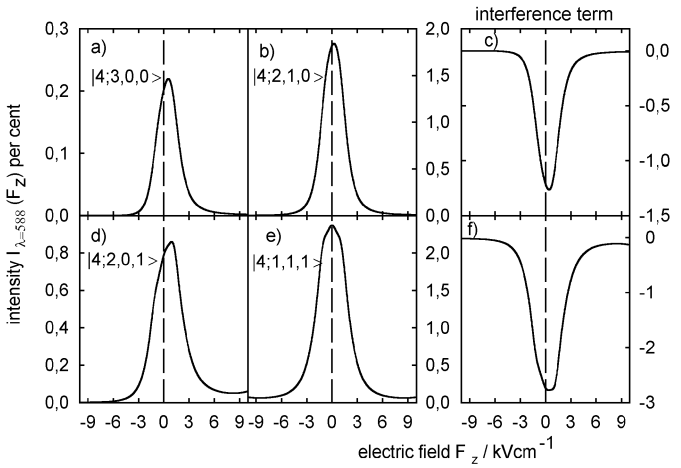

Fig. 3. The intensity function $I_{588}(F_z)$ of the $\lambda(1s3d\ ^3\mathrm{D}$–$1s2p\ ^3\mathrm{P}) = 588$ nm line calculated under the assumption that only one particular parabolic state $p = |n; n_1, n_2, |m|\rangle$ ($n = 4, |m| = 0, 1$) is populated and the emitted photon is polarized perpendicularly to the direction of observation. In the left column are shown the intensities for the states with maximal electric dipole moments ($n_2 = 0$), while in the middle column the intensities for the lower electric dipole moments ($n_2 = 1$) are represented. In the right column, are shown the intensities for the interference term resulting from coherent excitation of the states referred to in the first and second column. The diagonal elements of the excitation matrix σ are normalized to 100.

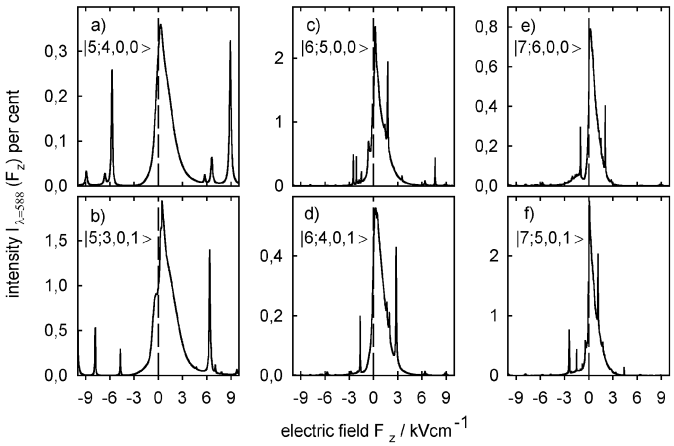

Fig. 4. The intensity function $I_{588}(F_z)$ of the $\lambda(1s3d\ ^3\mathrm{D}$–$1s2p\ ^3\mathrm{P}) = 588$ nm line calculated under the assumption that only one particular parabolic state $p = |n; n_1, n_2, |m|\rangle$ ($n = 5$, 6, 7 and $|m| = 0, 1$ is populated and the emitted photon is polarized perpendicularly to the direction of observation. There are shown the intensities only for the states with maximal electric dipole moments ($n_1 = n - 1, 2;\ n_2 = 0$). The diagonal elements of the excitation matrix σ are normalized to 100.

peak. A detailed comparison reveals, however, that besides direct excitation of $n = 4$ states also cascading from states with $n \geq 5$ contributes to the population of the $1s3d\ ^3\mathrm{D}$ level. On one hand, there are the small intensity maxima at electric fields of a few kV/cm, which can be related to singlet-triplet anticrossings of the $1s5l$ configurations. On the other hand, the narrow tip of the zero-field peak can only be reproduced by taking into account cascading from highly excited levels.

Figure 4 shows intensity functions calculated by assuming direct excitation of parabolic $n_2 = 0$ states with $n = 5$, 6 and 7. Since the polarizability of the excited He atoms increases, the widths of the zero-field peaks strongly decrease with increasing n. Also the intensity maxima due to singlet-triplet anticrossings become extremely narrow and occur at weaker electric fields.

Finally to reproduce qualitatively the experimental intensity function (Fig. 1, solid line), the following formula was used:

$$I_{588}^{\mathrm{det}}(F_z) = CI_{588}(F_z) + I^D, \tag{17}$$

where $I_{588}(F_z)$ is the calculated intensity function (16), C: normalization constant and I^D is the intensity of the dark current signal.

The only parameters left for reproducing the shape of the measured intensity function within the framework of the Paul-trap model are the relative population of the parabolic Σ and Π states with $n_2 = 0$ and the scaling of the excitation cross-sections with the principal quantum number n. Regarding the zero-field resonances, the signal shapes obtained for the Σ and Π states with $n_2 = 0$ (Figs. 3 and 4) are similar. However, Σ and Π give rise to different anticrossing resonances. Therefore, the population ratio

$$r^{(n)} = \mathrm{Tr}(\sigma^{n,\Sigma})/2\mathrm{Tr}(\sigma^{n,\Pi}) \tag{18}$$

can best be determined from the measured amplitudes of anticrossing resonances. For 12.5 keV-proton impact excitation of $n = 5$ states, Büttrich *et al.* [7] deduced $r^{(5)} = 1.5 \pm 0.1$. This result is also in agreement with the anticrossing amplitudes of the measured intensity function $I_{588}(F_z)$ shown in Figure 1, though a detailed comparison is complicated due to the broadening of the anticrossing resonances induced by the inhomogeneity of the electric field.

In accord with the experimental results [7,25,26] that similar anticrossing spectra were measured for $n = 4$, 5, 6 and 7, I assumed this Σ/Π population ratio $r^{(n)} = 1.5$ for all n shells. Finally an appropriate choice had to be made for the scaling of the excitation cross-sections with n. A satisfying agreement of the calculated intensity function $I_{588}(F_z)$ with the measured one was obtained using an n^{-3} scaling of the excitation cross-sections. This scaling law is well-known to be valid in the high-energy range, where the excitation cross-sections can be calculated using Born's approximation. The present analysis of the electric-field dependence of the intensity of the 588 nm line shows that the same scaling law can also be assumed at intermediate energies, where the excitation cross-sections of the $1snd\ ^1\mathrm{D}$ levels reach their absolute maximum.

Though the calculated intensity function, shown in Figure 1 (broken line) is in reasonable agreement with the experimental one (solid line), some deviations are obvious. These deviations can mainly be attributed to the inhomogeneity of the electric field applied to the collision volume, which was not taken into account in the calculations. Due to this inhomogeneity, in particular, the anticrossing resonances of the measured intensity function are significantly broadened. As a result, the experimental amplitudes of the $n = 5$ anticrossings of both Σ and Π sublevels (marked by σ and π, respectively, in Fig. 1) are much smaller than the calculated ones, and resonances of anticrossings of sublevels with $n = 6$ and 7 were not detected. Since the electric-field broadening is proportional to the field strength, the zero-field resonance is less affected by the inhomogeneity. Also here the deviations are most significant, where the field strength is largest.

5 Conclusions

The intensity function $I_{588}(F_z)$ measured for 12.5 keV-proton impact on helium atoms by Büttrich *et al.* [7] was analyzed theoretically. Since the singlet states of He I are populated selectively by proton impact, the triplet line at $\lambda(1s3d\ ^3\mathrm{D}–1s2p\ ^3\mathrm{P}) = 588$ nm appears only due to singlet-triplet mixing of high-l states. The theoretical analysis of the measured intensity function confirmed that at the intermediate proton energy of 12.5 keV, where the excitation functions of the $1snd\ ^1$D states exhibit a resonance-like maximum, the high-l states are populated in accordance with Paul-trap model and saddle dynamics: namely that within an n-shell the parabolic Σ and Π Stark sublevels with the largest electric dipole moments ($n_2 = 0$) are excited selectively. Furthermore, the measured intensity function is in agreement with the assumption that the excitation cross-sections $\sigma^{(n)}$ of different n-shells scale as n^{-3} in the intermediate energy range.

It would be worthwhile to investigate the intensity function $I_{588}(F_z)$ thoroughly in an extended energy range. Measurements on the anticrossing spectra of the $1s4d$ and $1s5d$ configurations [7,25] have shown that the excitation matrices change dramatically with increasing proton energy. In particular, referring to parabolic basis states, not only He I states with $n_2 = 0$, but also with $n_2 = 1$ are increasingly populated. Since the parabolic $n_2 = 0$ and $n_2 = 1$ states are populated partly coherently, this change of the excitation matrix significantly affects, in particular, the population of high-l states. Measurements of the intensity of the 588 nm line as a function of an electric field F_z would provide excellent means to analyze the variation of the high-l components of the excitation matrices with the proton energy.

I am grateful to Professor G. von Oppen for his support and stimulating discussions and for M.-J. Thuy for his valuable comments. This research was performed with the financial support from the University of Gdańsk (Grant BW 5200-5-0198-1).

References

1. A. Wolf, G. von Oppen, W.-D. Perschmann, D. Szostak, Z. Phys. A **292**, 319 (1979), and references therein
2. D.R. Cok, S.R. Lundeen, Phys. Rev. A **19**, 1830 (1979); Phys. Rev. A **24**, 3283 (1981)(E)
3. T.G. Eck, Phys. Rev. Lett. **31**, 270 (1973)
4. L.A. Sellin, J.R. Mowat, R.S. Peterson, P.M. Griffin, R. Laubert, H.H. Haselton, Phys. Rev. Lett. **31**, 1335 (1973)
5. C.C. Havener, N. Rouze, W.B. Westerveld, J.S. Risley, Phys. Rev. A **33**, 276 (1986)
6. A.S. Aynacioglu, G. von Oppen, R. Mller, Z. Phys. D **6**, 155 (1987)
7. S. Büttrich, D. Gildemeister, M.-J. Thuy, M. Tschersich, B. Skogvall, G. von Oppen, R. Drozdowski, J. Phys. B: At. Mol. Opt. Phys. **31**, 2709 (1998)
8. B. Skogvall, G. von Oppen, in *Selected Topics on Electron Physics*, edited by D.M. Campbell, H. Kleinpoppen (Plenum, New York, 1996), and references therein
9. S. Bttrich, G. von Oppen, Phys. Rev. Lett. **71**, 3778 (1993)
10. G. von Oppen, Europhys. Lett. **27**, 279 (1994)
11. G. von Oppen, M. Tschersich, B. Skogvall, R. Drozdowski, ARI **51**, 48 (1998)
12. G. von Oppen, M. Tschersich, R. Drozdowski, M. Busch, Aust. J. Phys. **52**, 431 (1999)
13. W. Paul, Phys. Blaett. **46**, 227 (1990)
14. J.M. Rost, J.S. Briggs, J. Phys. B: At. Mol. Opt. Phys. **24**, 4293 (1991)
15. H. Bethe, E. Salpeter, *Quantum Mechanics of one- and Two-Electron Atoms* (Springer, Berlin, 1957)
16. C.C. Havener, W.B. Westerveld, J.S. Risley, N.H. Tolk, J.C. Tully, Phys. Rev. Lett. **48**, 926 (1982)
17. S. Büttrich, Ph.D. thesis, TU Berlin, 1995
18. K. Blum, *Density Matrix Theory and Application* (Plenum Press, 1981)
19. E.W. Thomas, *Excitation in Heavy Particle collisions* (Wiley-Interscience, New York, 1972)
20. W.C. Martin, Phys. Rev. A **36**, 3575 (1987)
21. D. Kaiser, Ph.D. thesis, TU Berlin, 1993
22. D. Kaiser, Y.-Q. Liu, G. von Oppen, J. Phys. B: At. Mol. Opt. Phys. **26**, 363 (1993)
23. A. Kono, S. Hattori, Phys. Rev. A **29**, 2981 (1984)
24. W.C. Martin, J. Res. Natl. Bur. Stand. Sec. A **64**, 19 (1960)
25. R. Drozdowski, M.-J. Thuy, M. Tschersich, B. Skogvall, G. von Oppen, J. Phys. B: At. Mol. Opt. Phys. **32**, 397 (1999)
26. M. Tschersich, R. Drozdowski, M. Busch, B. Skogvall, G. von Oppen, J. Phys. B: At. Mol. Opt. Phys. **32**, 5539 (1999)